Anomalous Proximity Effect in Gold Coated (110) $YBa_2Cu_3O_{7-\delta}$ Films: Penetration of the Andreev Bound States

Itay Asulin,[1] Amos Sharoni,[1] Ofer Yulli,[1] Gad Koren,[2] and Oded Millo[1,*]

[1]*Racah Institute of Physics, The Hebrew University, Jerusalem 91904, Israel*
[2]*Department of Physics, Technion–Israel Institute of Technology, Haifa 32000, Israel*
(Received 30 May 2004; published 4 October 2004)

Scanning tunneling spectroscopy of (110)$YBa_2Cu_3O_{7-\delta}$/Au bilayers reveal a proximity effect markedly different from the conventional one. While proximity-induced mini-gaps rarely appear in the Au layer, the Andreev bound states clearly penetrate into the metal. Zero bias conductance peaks are measured on Au layers thinner than 7 nm with a magnitude similar to those detected on the bare superconductor films. The peaks then decay abruptly with Au thickness and disappear above 10 nm. This length is shorter than the normal coherence length and corresponds to the (ballistic) mean free path.

The mutual effect of a superconductor (*S*) in good electrical contact with a normal metal (*N*), a phenomenon known as the proximity effect (PE), is one of the most intriguing fundamental properties of superconductors that also yields various applications [1]. The PE has been studied extensively for conventional (*s*-wave) superconductors in contact with a normal metal. In such systems, an abrupt change in the pair potential, from a finite value on the *S* side to zero on the *N* side, leads to a smooth change of the pair amplitude, from its full bulk value deep in the *S* side to zero at a distance characterized by the normal coherence length, ξ_n [1–5]. The pair amplitude is proportional to the gap in the quasiparticle density of states (DOS) and can thus be monitored by tunneling spectroscopy.

For an anisotropic *d*-wave superconductor, the crystallographic orientation of the superconductor surface at the *N*-*S* interface can significantly modify the PE. Sharoni *et al.* [6] have shown, using gold-coated *c*-axis $YBa_2Cu_3O_{7-\delta}$ (YBCO) samples, that the PE is primarily due to the interface between the normal metal and the (100) YBCO surface, whereas virtually no effect is pertained to the (001) surface. This facet selectivity reflects the in plane versus out of plane anisotropy in the cuprate superconductors, which was also measured indirectly by other groups [7–9]. However, the proximity-induced order parameter decayed exponentially in a way typical of conventional *N*-*S* proximity systems. In particular, the measured normal coherence length, ~ 30 nm, agrees with the dirty limit approximation, $\xi_N = (\frac{\hbar v_N l_N}{6\pi k_B T})^{1/2}$, assuming that the mean free path is governed by grain-boundary scattering, $l_N \sim 10$ nm, in the corresponding gold layer. In addition, the induced order parameter appeared to have *s*-wave symmetry.

The *d*-wave symmetry of the pair potential in YBCO should also lead to anisotropy in the *S*-*N* PE for different crystallographic orientations within the *a*-*b* plain,

mainly between antinodal and nodal surfaces [10–12]. According to some theoretical calculations, no conventional PE is expected for junctions involving the nodal (110) YBCO surface [12]. In particular, no penetration of the pair amplitude into the *N* side, which leads to the appearance of "minigaps" [3–6] in the DOS, is predicted. Recent circuit theory models suggest that zero energy Andreev bound state (ABS) channels quench the PE in the nodal direction [10,11], since electrons can enter *S* and *uncorrelated* electron-hole pairs can penetrate *N* through the ABS channels. However, a clear picture of the spatial variation of the DOS in the vicinity of these junctions, in particular, the (possible) penetration of the ABS into the *N* layer has not yet been established. Resolving these issues, which is the main focus of the present Letter, is important for gaining a better understanding of both the PE involving *d*-wave superconductors and the nature of the ABS.

As mentioned above, ABS appear on the nodal surfaces of *d*-wave superconductors [13–16]. These states result from the pair breaking nature of nodal surfaces (introducing an effective thin *N* layer) [13], and the *d*-wave pair potential sign inversion felt by the Andreev reflected quasiparticles. An intriguing question that has not yet been examined is how the ABS propagate into a normal metal layer that is deposited onto the nodal *S* surface. One can speculate that as long as the trajectories of the quasiparticles are momentum and phase coherent and the relevant interfaces are specular, ABS should reside in the *N* layer [13]. The question regarding how their spectral strength would evolve with the normal layer thickness has not yet been treated, either theoretically or experimentally.

In this work, we studied the PE in nodal (110) epitaxial thin films of YBCO covered with gold layers of various thicknesses. Gap shaped tunneling spectra were sporadically measured with no clear dependence on Au thick-

ness. [One should bear in mind, however, that (100) facets were scarce in these YBCO films.] At the same time, our tunneling spectra clearly revealed, for the first time, a penetration of the ABS into N, appearing as zero bias conductance peaks (ZBCP) in the tunneling spectra. The penetration depth was much shorter as compared to that observed for the order parameter (energy gap) in (100)YBCO/Au junctions [6]. Moreover, the ZBCP did not decay exponentially but appeared to be nearly constant for Au thicknesses of up to ~ 7 nm. Above this, the ZBCP decayed rapidly and was not detected at all on Au layers thicker than 10 nm. The small abundance of gaps, on one hand, and the unique behavior of the ZBCP, on the other, point out to an unconventional PE in S-N junctions involving nodal d-wave surfaces.

A total of 22 bare and gold-coated (110)YBCO samples were measured, with Au thickness values ranging up to 30 nm. The (110)YBCO/Au bilayers were prepared by laser ablation deposition on (110) SrTiO$_3$ wafers. First, a 10 nm thick template layer of YBCO was deposited at $660\,^\circ$C substrate temperature to ensure an undisturbed (110) orientation. Subsequently, the temperature was raised to $760\,^\circ$C, and a 50 nm thick YBCO film was prepared, maintaining the (110) orientation. The temperature was then lowered to $450\,^\circ$C in 50 Torr of oxygen pressure, and the film was left for oxygen intake at this temperature for 1 h. Later on, the gold layer was deposited *in situ* at $200\,^\circ$C and annealed in 250 Torr of oxygen pressure at this temperature for about 2 h. X-ray diffraction analysis showed that the YBCO films are oriented in the (110) direction, with less than 5% of other orientations. The transition temperatures of our films were around 88 K with a relatively narrow transition width of 2 K, implying slightly underdoped homogeneous films.

The STM data presented here were all acquired at 4.2 K using a (normal metal) Pt-Ir tip. The tunneling spectra (dI/dV vs V characteristics, proportional to the local quasiparticle DOS) were obtained by numerical differentiation of I-V curves taken while momentarily disconnecting the feedback loop. The spectra were taken at specific well-defined locations correlated with the surface
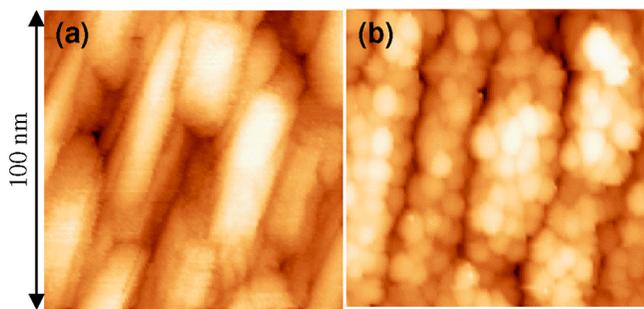
topography. Several I-V curves were acquired at each position to ensure data reproducibility. The voltage and current settings (i.e., the tip-sample distance) had no influence on the main spectral features, ruling out the possible contributions of single electron charging effects [17].

STM and atomic-force microscopy measurements of the bare YBCO films revealed $\sim 40 \times 100$ nm^2 elongated crystallite structures about 4 nm in height. The crystallites had uniform directionality, parallel to the (110) side of the SrTiO$_3$ wafer, over areas of a few μm^2, as portrayed in Fig. 1(a). This structure is consistent with twinning of our YBCO films. The elongated crystallite structure was clearly visible even after deposition of the thickest gold layer (30 nm). Figure 1(b) presents a YBCO film coated with a 7 nm thick gold layer, clearly showing both the finer Au granularity and the elongated crystallite structure of the underlying YBCO film. The figure also shows that the gold layer fully covered the YBCO film and the surface morphology revealed grains with lateral size of 10 nm and rms height roughness of less than 1.5 nm. We note that after annealing, good coverage (with no apparent "pin holes") was achieved for gold films of average thickness larger than 3–4 nm.

The bare samples exhibited pronounced ZBCP in the tunneling spectra over large areas, indicative of a dominant (110) surface orientation. In addition to the ZBCP, the spectra also show gaplike features at approximately 10 meV, as well as an asymmetry between the negative and positive bias. A correlated topography-spectroscopy mea-
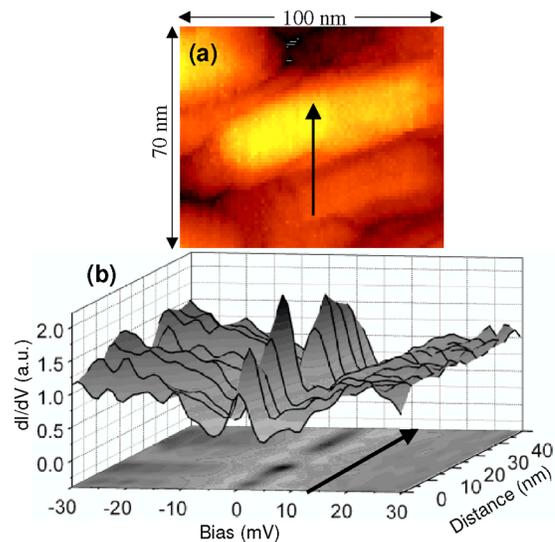
FIG. 2 (color online).   STM measurement demonstrating the spatial evolution of the ZBCP on the bare YBCO films. (a) Topographic image, featuring two adjacent YBCO crystallites (possibly twins). (b) Tunneling spectra taken along the arrow marked in (a). The projection of the spectra (in gray scale) onto the XY plane clearly portrays the vanishing of the ZBCP near the boundary and its nearly constant width.

FIG. 1 (color online).   STM topographic images of (a) a bare (110) YBCO surface and (b) 7 nm (nominal) gold film coating a similar YBCO sample.

surement manifesting the spatial changes of the ZBCP on the bare YBCO films is presented in Fig. 2. Figure 2(a) presents a topographic image of a bare YBCO film, focusing on two adjacent crystallites. The tunneling spectra shown in Fig. 2(b) were sequentially obtained at fixed steps along the arrow marked in Fig. 2(a). Evidently, the ZBCP (thus, also the ABS) exhibit spatial continuity over the YBCO crystallite but vanish in the vicinity of the (possibly twin) boundary (and other surface imperfections). This may be due to the formation of a thin disordered layer near the boundaries, in which the d-wave order parameter is strongly reduced and, in particular, the ZBCP is smeared out [18,19]. Interestingly, the ZBCP appears to recover over a length scale that is comparable to the YBCO coherence length, ~2 nm. Note that the ZBCP had a nearly fixed width, independent of its amplitude and the point of acquisition, in agreement with previous reports [16,20].

The ZBCP appeared not only on the bare YBCO film, but also on samples with thin gold coating, featuring the same spatial variation as in the bare films, as demonstrated in Fig. 3. Figure 3(a) presents a topographic image of a 7 nm YBCO/Au bilayer, showing, again, full coverage of the Au film. The tunneling spectra presented in Fig. 3(b) were taken along the white arrow marked in Fig. 3(a), spanning a full cross section of a single crystallite. The ZBCP were observed all over the YBCO crystallite, on and between gold grains, with mild fluctuations in height. However, it vanished at the crystallite boundaries, thus replicating the behavior observed on the bare YBCO films.
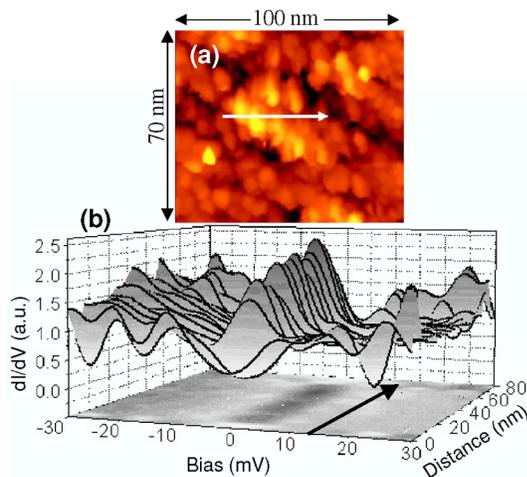

FIG. 3 (color online). Spatial evolution of the ZBCP in a (110)YBCO/7 nm gold bilayer. (a) Topographic image where the structure of the underlying YBCO crystallite is clearly visible. (b) Tunneling spectra measured along the white arrow spanning a full width of a crystallite. The ZBCP is continuous over the full width of the YBCO crystallite, with mild fluctuation, and disappears at the edges (evident in the projection onto the XY plane).

In order to quantitatively compare the ZBCP amplitude between samples of different gold layer thickness, we applied the following procedure for calculating the area of the peak, which is a measure of the density of ABS. The ZBCP was first normalized by the normal conductance background well above the superconducting gap, at a bias voltage of around $+30$ mV. Then the area between the ZBCP and its base was integrated as illustrated in the inset of Fig. 4.

Figure 4 shows the integrated ZBCP area (proportional to the number of ABS) as a function of the gold layer thickness, i.e., the distance from the N-S interface. This plot depicts a behavior that is markedly different from an exponential decay expected for conventional proximity systems [1]. An exponential decay was observed also for the (100)YBCO/Au interface by Sharoni et al. [6]. The magnitude of the ZBCP in Fig. 4 appears to be rather constant for gold layers of thickness up to ~7 nm, and decays abruptly above that. In particular, the ABS vanished 10 nm away from the (110)YBCO/Au interface, in contrast to the (100)YBCO/Au interface, where proximity-induced energy gaps were still clearly observed at distances larger than 30 nm away from it [6]. We note here that the gold layers had a similar morphology in both cases. The large vertical error bars in Fig. 4 reflect the extreme sensitivity of the ZBCP amplitude to the local spatial variations of the disorder in the gold and the YBCO films, and the specularity of the interface (for instance, the sample with 9.5 nm gold thickness showed large areas free of ZBCP).

In order to better understand our results we recall that the mean free path in our gold films is determined by grain-boundary scattering and is around 10 nm [6]. This implies that as long as the normal layer is shorter than the mean free path, it does not have much effect on the
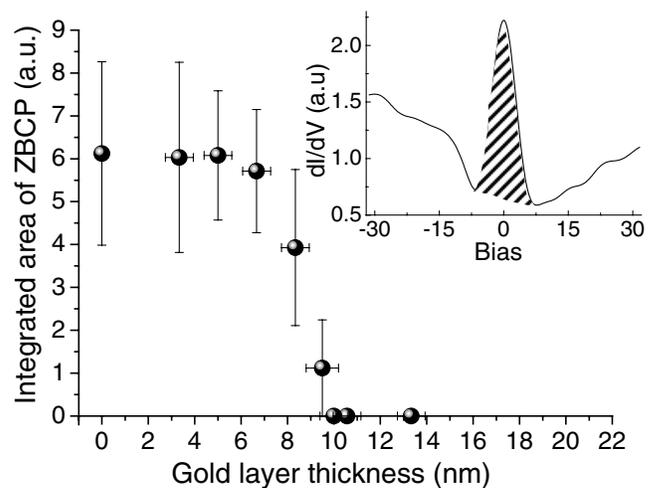

FIG. 4. The normalized ZBCP integrated area as a function of nominal gold layer thickness. The inset depicts the integrated area of the normalized peak.

density of ABS, as predicted by Hu [13]. Namely, the penetration range of the ZBCP is determined by the "ballistic" mean free path, in contrast to the penetration range of the order parameter which was found to coincide with the thermal (or phase coherence) length, $\xi_N = (\frac{\hbar v_N l_N}{6\pi k_B T})^{1/2}$. We note in passing that Fig. 2 displays a third characteristic length, the coherence length in YBCO, ~ 2 nm, which determines the range over which the ZBCP recovers away from an imperfection on the (110)YBCO surface. In addition to the ZBCP, we also measured spectra exhibiting minigaps. These gaps were occasionally observed only on rather small portions of the gold-coated films. Their size did not show any clear correlation with the thickness of the Au layer, nor with any apparent morphological feature. They may be associated with (100)YBCO nanofacets (such as in Ref. [6]) that are masked in the topographic images by the Au coating. The short length scale (smaller than ξ_N and of the order of l_N) over which the ZBCP persists in the normal layer, and the sporadic nature of the detected minigaps, point to an unconventional PE in S-N bilayers involving the nodal surface of a d-wave superconductor. The PE manifests itself via a unique appearance of the ZBCP on the N surface, as demonstrated in Fig. 4.

The formation of bound states in a proximity S-N system that give rise to the ZBCP measured on the N side requires several conditions. First, the S-N interface should be transparent in order to allow Andreev reflections. This condition is satisfied in our samples due to the *in situ* deposition and the postannealing of the gold layer. The second condition is having phase coherence between the electron and hole over their trajectories in the normal layer [13]. This requirement is obviously maintained in our case, since the corresponding coherence length was found to be 30 nm [6], larger than the scale over which the ZBCPs were observed here. The last requirement, which is related to the properties of the Au film, is having specular reflection at the gold surface and electron and hole momentum conservation within it [13,21,22]. The latter condition should hold for gold layers thinner than l_N (the grain size in our case), consistent with our observation for the penetration depth of ~ 10 nm. However, the unique thickness dependence of the ZBCP, exhibiting a nonexponential decay unlike diffusive systems, still needs to be explained. For this we need one of the above conditions to fail abruptly. Possibly, due to the narrow distribution of the gold grain size (as evident from our morphological analysis of the gold layers), there is a well-defined length scale for momentum conservation breaking, resulting in a rapid decay of the ZBCP amplitude. We note here that reminiscent ballistic effects were also detected in conventional Nb-Au proximity systems [23].

In summary, our scanning tunneling spectroscopy of (110)YBCO/Au bilayers features an anomalous PE. A minigap structure, typical of S-N proximity systems, was not induced. ABSs, however, clearly penetrate the gold layer, but only over a short length determined by the mean free path, ~ 10 nm, which is much shorter than the normal coherence length. The amplitude of the corresponding ZBCP decays with gold layer thickness in a unique nonexponential way, typical of an order parameter in diffusive proximity systems. Rather, the amplitude is nearly constant up to a gold layer thickness of 7 nm and then decays abruptly, signifying a ballistic effect.

*Electronic address: milode@vms.huji.ac.il

[1] G. Deutscher and P. G. De Gennes, *Superconductivity* (Marcel Dekker, Inc., New York, 1969).
[2] Y. Levi *et al.*, Phys. Rev. B **58**, 15 128 (1998).
[3] N. Moussy, H. Courtois, and B. Pannetier, Europhys. Lett. **55**, 861 (2001).
[4] W. Belzig, C. Bruder, and G. Schon, Phys. Rev. B **54**, 9443 (1996).
[5] S. Gueron *et al.*, Phys. Rev. Lett. **77**, 3025 (1996).
[6] A. Sharoni *et al.*, Phys. Rev. Lett. **92**, 017003 (2004).
[7] M. Lee *et al.*, Appl. Phys. Lett. **57**, 1152 (1990).
[8] M. A. M. Gijs *et al.*, Appl. Phys. Lett. **57**, 2600 (1990).
[9] H. Z. Durusoy *et al.*, Physica (Amsterdam) **266C**, 253 (1996).
[10] Y. Tanaka *et al.*, Phys. Rev. B **69**, 144519 (2004).
[11] Y. Tanaka, Y. V. Nazarov, and S. Kashiwaya, Phys. Rev. Lett. **90**, 167003 (2003).
[12] Y. Ohashi, J. Phys. Soc. Jpn. **65**, 823 (1996).
[13] C. R. Hu, Phys. Rev. Lett. **72**, 1526 (1994).
[14] Y. Tanaka and S. Kashiwaya, Phys. Rev. Lett. **74**, 3451 (1995).
[15] A. Sharoni, G. Koren, and O. Millo, Europhys. Lett. **54**, 675 (2001).
[16] L. Alff *et al.*, Phys. Rev. B **55**, R14 757 (1997).
[17] E. Bar-Sadeh *et al.*, Phys. Rev. B **53**, 3482 (1996).
[18] J. X. Zhu *et al.*, Phys. Rev. Lett. **91**, 057004 (2003).
[19] A. A. Golubov and M. Y. Kupriyanov, Superlattices Microstruct. **25**, 949 (1999).
[20] M. B. Walker and P. Pairor, Phys. Rev. B **60**, 10 395 (1999).
[21] M. Fogelstrom, D. Rainer, and J. A. Sauls, Phys. Rev. Lett. **79**, 281 (1997).
[22] Y. Asano and Y. Tanaka, Phys. Rev. B **65**, 064522 (2002).
[23] A. K. Gupta *et al.*, Phys. Rev. B **69**, 104514 (2004).